ELSEVIER

Journal of Magnetism and Magnetic Materials 198–199 (1999) 396–401

Journal of magnetism and magnetic materials

Invited paper

Exchange coupling in magnetic multilayers grown on iron whiskers

J. Unguris*, R.J. Celotta, D.A. Tulchinsky, D.T. Pierce

Electron Physics Group, National Institute of Standards and Technology, Building 220, Room B206, Gaithersburg, MD 20899, USA

Abstract

Meaningful tests of theoretical predictions of magnetic multilayer properties require the fabrication of multilayers with nearly the same atomic scale precision as the theoretical models. Multilayers grown epitaxially on single-crystal Fe whisker substrates come very close to this ideal standard. We have investigated the growth, magnetic structure, and exchange coupling of Fe/(Ag, Au, Cr, Mn, V, Cu, or Al)/Fe (1 1 0) whisker structures primarily using reflection high-energy electron diffraction (RHEED) and scanning electron microscopy with polarization analysis (SEMPA), and in some systems, confocal magneto-optic Kerr effect (MOKE) microscopy. In cases of nearly layer-by-layer growth, the measured oscillatory coupling periods and strengths agree well with theoretical predictions. For rougher growth, less predictable non-collinear coupling is generally observed.

Keywords: Interlayer exchange coupling; Magnetic multilayers; SEMPA; Magnetic microstructure; Spin density waves

1. Introduction

In certain cases, growing magnetic multilayers on Fe whisker substrates has achieved the nearly perfect atomic ordering required to make meaningful comparisons to theories of magnetic exchange coupling. Exchange coupling measurements of Fe multilayers with Ag [1], Au [2,3], or Cr [4] interlayers grown on Fe whiskers have shown that many of the discrepancies between experiment and theory can be resolved by removing or quantifying the atomic scale disorder in the multilayer. We have examined several other potential interlayer materials and extended some of our earlier measurements on Cr. This paper summarizes our results for these various spacer layers.

2. Experimental

An essential ingredient in all of these experiments is the Fe whisker substrate. These whiskers, grown by thermal decomposition of $FeCl_2$ in an H_2 atmosphere, are among the most perfect metal crystals known [5]. More importantly for thin film growth, nearly perfect (1 0 0) surfaces can simply be obtained by in situ ion sputtering and thermal annealing [6]. Scanning tunneling microscopy (STM) measurements of these surfaces reveal step densities of a single atomic step per micrometer over hundreds of micrometers [7]. Reflection high-energy electron diffraction (RHEED) patterns consist of very sharp diffraction spots with no streaking and minimal diffuse scattering. The whiskers used in these measurements were about 10 m long, a few tenths of a mm wide, and had a rectangular cross section that stabilized the magnetic structure into two opposite domains.

The samples were prepared and measured following procedures described previously [4,6,8]. Fig. 1 shows a schematic diagram of the sample configuration and an example of a scanning electron microscopy with polarization analysis (SEMPA) measurement from an Fe/Au/Fe sample. Wedge-shaped interlayers are grown in order to investigate the exchange coupling as a function of spacer layer thickness. Typical wedge slopes were about 1 atom layer per 10 μm. SEMPA measurements were made before, during and after Fe deposition.

*Corresponding author. Tel.: +1-301-975-3712; fax: +1-301-926-2746.

E-mail address: unguris@epg.nist.gov (J. Unguris)

0304-8853/99/$ – see front matter
PII: S0304-8853(98)01139-1

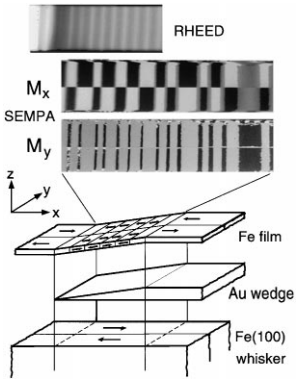

Fig. 1. (Bottom) Schematic diagram of the sample configuration consisting of the Fe (0 0 1) whisker, a wedge-shaped spacer layer (Au in this example), and a thin Fe top layer. (Top) The top image shows the spatial RHEED intensity oscillation measurement of the spacer which provides a precise measure of the spacer thickness. The SEMPA images show two components of the magnetization, M_x and M_y, where white (black) indicates magnetization in the positve (negative) x- or y-direction along and across the whisker, respectively.

RHEED, both in time-resolved and spatially-resolved modes, was used to monitor the quality of the film growth and to measure the thickness of the films. Fig. 1 shows a RHEED image of the Au wedge before coating with Fe.

3. Results

The growth of the various interlayer materials on the Fe whisker substrates is summarized by the thickness-dependent RHEED scans shown in Fig. 2. The films were grown at the temperatures indicated. Cr, Ag and Au grow nearly layer-by-layer and provide the best measurements of oscillatory exchange coupling. The exchange coupling for these spacer layers along with Mn and V is summarized by the M_x line scans shown in Fig. 3. The oscillatory exchange coupling periods derived from these measurements are summarized and compared to theory [9–12] in Table 1. Mn, V, Al and Cu all grow following different variations of Stranski–Krastanov growth modes; growing layer-by-layer initially and then switching to rough or three-dimensional growth at some critical thickness.

3.1. Cr

Although Fe/Cr/Fe was the first multilayer in which oscillatory exchange coupling was observed, it continues to be an interesting system due to the rich variety of possible Cr magnetic states. The highest quality Cr films are grown at elevated temperatures of about 300–350°C.

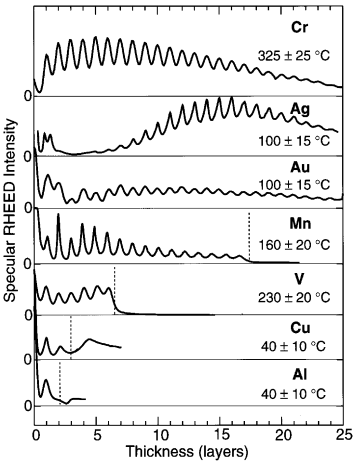

Fig. 2. RHEED intensity oscillations as a function of thickness for deposition of the various materials on to the Fe substrate at the temperatures indicated. The dashed lines show the abrupt change to rough or 3-d growth.

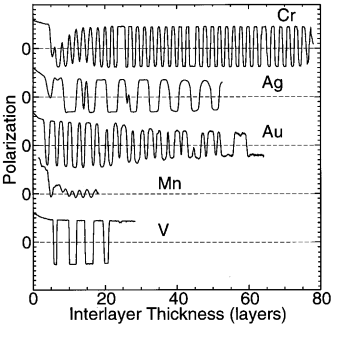

Fig. 3. Polarization line scans from SEMPA images showing oscillations of M_x in the top Fe layer as a function of the spacer layer thickness.

This high-temperature growth can lead to alloying at the Cr/Fe interface [13,14], but growing the first two Cr layers at a lower temperature of about 100°C minimizes the interfacial alloying and increases the magnitude of the Fe/Cr/Fe exchange coupling strength [15]. SEMPA measurements of Fe/Cr/Fe coupling on Fe whiskers, such as the one shown in Fig. 3, show nearly layer-by-layer switching between ferromagnetic and antiferromagnetic alignment for almost 80 layers of Cr [8,16]. Closer inspection of the SEMPA data actually reveals that two coupling periods are present; there is a strong short period nearly commensurate with the lattice and a longer period. Which of these periods is dominant depends sensitively on the thickness fluctuations in the Cr spacer layer as has been verified by STM measurements [17]. SEMPA measurements of only bare Cr on the Fe whisker also reveal the same short period oscillations

Table 1
The measured periods for coupling in the [0 0 1] direction for Cr, Ag, Au, and V are compared to theory. Except for V where the growth is poor, there is excellent agreement with the predictions of theory

Interlayer	Measured	Theory		
		Stiles [9,10]	Bruno and Chappert [11]	Van Schilfgaarde and Herman [12]
Cr (0.144 nm/layer)	2.105 ± 0.005	2.10		2.15
	12 ± 1	11.1		12.3
Ag (0.204 nm/layer)	2.37 ± 0.07	2.45	2.38	
	5.73 ± 0.05	6.08	5.58	
Au (0.204 nm/layer)	2.48 ± 0.05	2.50	2.51	
	8.6 ± 0.3	9.36	8.60	
V (0.152 nm/layer)	~ 5			3.08
				11.0

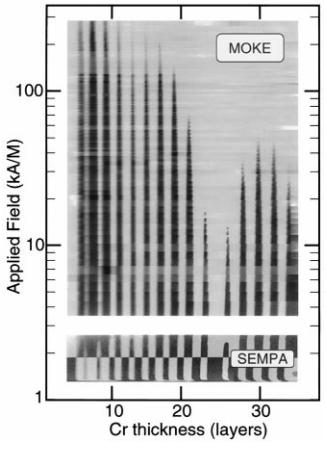

Fig. 4. A series of MOKE images from an Au (10 ML)/Fe(15 ML)/Cr wedge/Fe whisker sample taken at various applied magnetic fields, showing the field and Cr thickness dependence of the reversal of the antiferromagnetic regions (dark bands). The Fe/Cr/Fe exchange coupling strength is determined from the switching field. A SEMPA image of the same wedge at zero applied field is shown at the bottom for reference.

[16]. For both bare Cr and Fe coated Cr, the incommensurate short-period oscillations result in phase slips in the coupling at about 24, 44 and 64 layers at room temperature owing to the slight difference between the lattice wave vector and Fermi surface spanning vector.

Further evidence for the incommensurate nature of the short-period coupling is also seen in the magneto-optic Kerr effect (MOKE) measurements shown in Fig. 4. The figure consist of a series of MOKE images of the Fe/Cr/Fe (1 0 0) wedge taken at various applied magnetic fields. This series of images graphically shows how the strength of the antiferromagnetic exchange coupling depends on the Cr thickness. These measurements clearly show the incommensurate spin density wave nature of the Cr with the expected minimum in the coupling strength at the position of the phase slip at 24 layers [18,19]. This figure also shows how difficult measuring coupling strengths of well-ordered Fe/Cr/Fe structures one thickness at a time can be: a change in the Cr thickness of only a tenth of a monolayer can lead to over an order of magnitude change in the exchange coupling strength.

The incommensurate short-period oscillations along with the related phase slips are also very sensitive to temperature. Previous SEMPA measurements [16] of the bare Cr polarization show that the short-period oscillations exist to at least 1.8 times the bulk Néel temperature, $T_N = 311$ K. Fig. 5 shows a series of SEMPA measurements of the Fe/Cr/Fe coupling as a function of temperature. Fig. 5 also includes curves showing the thickness at which the phase slips in bare Cr/Fe occur. Like the Cr/Fe case, the short-period oscillations in Fe/Cr/Fe exist to nearly twice the bulk T_N and the phase slips have nearly the same temperature dependence. Locating the phase slip is somewhat difficult in Fe/Cr/Fe because the short-period coupling strength appears to drop off more rapidly with temperature than that of the long period. (Only the short-period oscillations are visible in the bare Cr/Fe data.) Note that all of these observations are completely reversible and are not due to an irreversible roughening of the multilayer. The temperature dependence of the coupling leads to reversals in the direction of the coupling i.e., below 420 K the coupling at 30 layers is antiferromagnetic, while above 500 K the coupling switches to ferromagnetic.

Our measurements are qualitatively similar to neutron scattering measurements which find a commensurate spin density wave below and incommensurate spin density wave above the first phase slip [20,21]. However, the

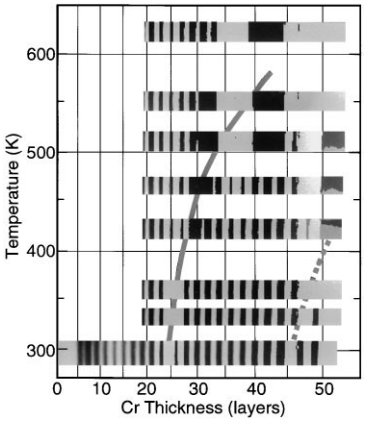

Fig. 5. The temperature dependence of the bilinear (M_x) exchange coupling in Fe/Cr/Fe. The phase slips measured on bare Cr are shown by the solid gray line; the dashed line is the estimated position of the next phase slip. Note that the short-period oscillations, where visible, have opposite direction at temperatures below and above these lines.

boundary dividing the two regions of spin density wave behavior saturates at about 300 K in the neutron measurements but extends to well over 500 K for our samples as seen in Fig. 5. The difference probably can be attributed to differences in crystalline order, lattice constants, or lattice strains in samples prepared in different ways and on different substrates.

3.2. Au and Ag

Although FCC Ag and Au have very different unit cells than BCC Fe, there is little lateral mismatch between the BCC substrate and the FCC overlayer when rotated by 45°. A large vertical mismatch remains, however, which can be a problem at substrate Fe steps. Both Ag and Au grow nearly layer by layer up to $\sim$50 layers, although each system has its own peculiarities: Au grows with a five-fold reconstruction of the top layer [2], while Ag seems to require an initial incubation period of between 2 and 6 layers before growing layer by layer [1]. SEMPA measurements of Ag and Au each reveal two coupling periods (see Table 1). The periods arise from the 'belly' and 'neck' extremal spanning vectors of the Fermi Surface of these noble metals. As can be seen in Fig. 3 the short period dominates the coupling in Au, while the longer period is strongest in Ag. The magnitude of the exchange coupling strength for Fe/Au/Fe whiskers has been measured by MOKE and found to be much larger than earlier measurements using non-whisker substrates. In fact, when the residual thickness fluctuations of the Au spacer layer are taken into account, the measured coupling strengths [3] are very close to the theoretically predicted values [22].

3.3. V

Vanadium grows in a Stranski–Krastanov mode with the first six layers growing layer by layer and then abruptly switching to rougher island growth for thicker films. The same growth behavior with roughening starting after exactly six layers was observed for various flux rates and for substrate temperatures ranging from 30° to 300°C. SEMPA measurements of an Fe/V/Fe wedge are shown in Fig. 6. For up to 20 layers the exchange coupling oscillates, but the growth is sufficiently rough to filter out any potential short-period oscillations. After 20 layers no coupling oscillations are observed. From this limited data it is difficult to derive precise oscillatory coupling periods. An average period of about 5 ± 1 layers may be estimated from the measurements. This value is different from calculated periods [12], but it is about the same as the 6 layer period observed by Parkin [23] for sputtered V/Co multilayers.

3.4. Mn

Although Mn is notable for its many different structural and magnetic phases, it appears to grow on Fe whiskers as a simple antiferromagnet with a bct structure closely matched to the substrate [24]. RHEED measurements show initial well-ordered layer-by-layer growth in the first few layers that gradually becomes rougher and finally, abruptly switches to 3-d growth after 15–20 layers. SEMPA measurements of the bare Mn wedge show an oscillating surface moment that is collinear with the Fe moment and consistent with antiferromagnetic Mn. While the bare Mn polarization is similar to that of Cr, the Fe/Mn/Fe exchange coupling is completely different. SEMPA measurements of the Fe/Mn/Fe wedge, Fig. 7, show that the coupling is oscillatory, but not collinear. After an initial transient phase for thin Mn films the coupling oscillates with a 2 layer period about 90° with respect to the Fe whisker magnetization. The magnitude of the oscillations varies for different Fe whisker substrates but is generally between 10 and 30°,

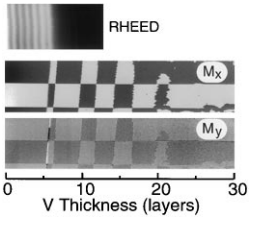

Fig. 6. The RHEED intensity imge shows that V grows nearly layer-by-layer for 6 layers. The SEMPA images show exchange coupling oscillations with a period of approximately 5 layers up to about 20 layers.

i.e. for the 10° amplitude the coupling oscillates between 80 and 100° [25].

3.5. Al

Aluminum is as well lattice matched to Fe (1 0 0) as are Ag or Au so that one might expect similar smooth, layer-by-layer growth, but instead Al forms rough three-dimensional films on Fe whisker substrates, and the exchange coupling is altered dramatically. Fig. 8 shows SEMPA and RHEED measurements for Al grown on an Fe whisker. For less than two Al layers, RHEED patterns indicate that the growth is smooth and epitaxial, and SEMPA images show that the Fe/Al/Fe is coupled ferromagnetically. For Al coverages greater than 3 layers, the RHEED patterns switch from sharp spots along an arc to a lattice of spots characteristic of transmission through three-dimensional Al structures. The dramatic roughening at such low Al coverages may indicate that the roughness is not just due to Al, but the Fe substrate may also become rougher as a result of the tendency of Al and Fe to form compounds. SEMPA images show that the coupling switches dramatically from ferromagnetic to a 90° alignment when the film becomes rough. Unlike earlier measurements by Fuss et al. [26], no antiferromagnetic coupling is observed, but the 90° biquadratic coupling agrees with the observations of Filipkowski et al. [27]. Neither of these other measurements used single-crystal Fe substrates however.

3.6. Cu

Copper does not lattice match well to the Fe (1 0 0) substrate and achieving layer-by-layer growth of Cu on an Fe whisker is consequently very difficult. We found that one or perhaps two layers of two-dimensional Cu could be grown epitaxially on the Fe (1 0 0) surface. Subsequent layers were not stable and formed three-dimensional bulk Cu crystallites at nucleation sites along the edge of the whisker or in regions that were not sputter cleaned. A surprising feature of this rough growth was the extreme mobility of the Cu deposited on 1–2 ML of Cu. Even at room temperature Cu diffused over relatively large distances, on the order of tenths of a mm, so that it could find nucleation sites and grow into crystallites. Fig. 9 shows SEM images from an uncleaned part of an Fe whisker in which several of these crystallites formed. No Cu crystallites were observed on the cleaned surface of the Fe whisker. Although the extreme mobility of the Cu on the Fe whisker is interesting, it prevented us from making any meaningful exchange coupling measurements on this system.

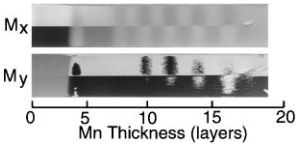

Fig. 7. The magnetization of the top Fe layer in Fe/Mn/Fe is oriented predominantly at right angles to the whisker magnetization. The contrast in the M_x image indicates a small oscillation of the magnetization about 90° with a period of 2 layers.

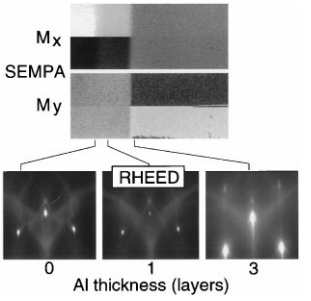

Fig. 8. RHEED images showing an arc of sharp spots for clean Fe and 1 layer of Al. By three layers of Al a 3-d transmission pattern is observed and the top Fe layer couples at 90° to the Fe whisker magnetization.

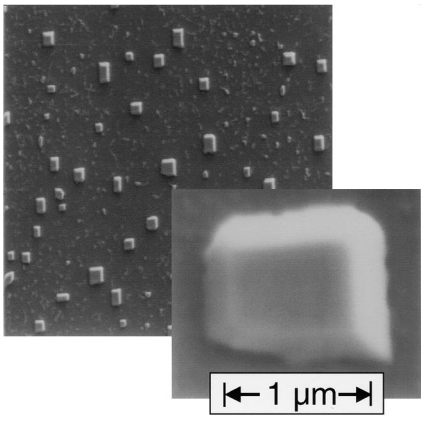

Fig. 9. The SEM image of Cu deposited on a Fe whisker showing the formation of 3-d Cu crystallites at nucleation sites.

4. Conclusions

Model epitaxial trilayer systems with Fe (0 0 1) whisker substrates were prepared to test theories of interlayer exchange coupling. Although structures with V, Mn, Al, and Cu exhibited some interesting properties, the quality of the growth was inadequate for a comparison of the observed coupling to theory. The Fe/Cr/Fe system continues to provide fascinating results. The strength of the coupling displays a minimum at the phase slip at 24

layers where a node is introduced into the spin density wave. Further, this phase slip boundary extends to temperatures nearly twice the bulk Néel temperature in contrast to neutron scattering measurements on samples with less perfect interfaces. The excellent agreement obtained between experiment and theory for the periods of the exchange coupling oscillations for Au, Ag, and Cr, and in the case of Au for the strength of the coupling as well, show that the theory of interlayer exchange coupling is now on sound footing.

Acknowledgements

We wish to thank Bret Heinrich and coworkers for initially supplying us with Fe whiskers and then teaching us how to grow them ourselves. This work was supported in part by the Office of Naval Research.

References

[1] J. Unguris, R.J. Celotta, D.T. Pierce, J. Magn. Magn. Mater. 127 (1993) 205.
[2] J. Unguris, R.J. Celotta, D.T. Pierce, J. Appl. Phys. 75 (1994) 6437.
[3] J. Unguris, R.J. Celotta, D.T. Pierce, Phys. Rev. Lett. 79 (1997) 2734.
[4] J. Unguris, R.J. Celotta, D.T. Pierce, Phys. Rev. Lett. 67 (1991) 140.
[5] S.S. Brenner, in: J.J. Gilman (Ed.), The Art and Science of Growing Crystals, Wiley, New York, 1963, p. 30.
[6] A.S. Arrott, B. Heinrich, S.T. Purcell, in: M.G. Lagally (Ed.), Kinetics of Ordering and Growth at Surfaces, Plenum, New York, 1990, p. 321.
[7] J.A. Stroscio, D.T. Pierce, J. Vac. Sci. Technol. B 12 (1994) 1783.
[8] D.T. Pierce, J. Unguris, R.J. Celotta, in: B. Heinrich, J.A.C. Bland (Eds.), Ultrathin Magnetic Structures II, Springer, Berlin, 1994, p. 117.
[9] M.D. Stiles, Phys. Rev. B 48 (1993) 7238.
[10] M.D. Stiles, Phys. Rev. B 54 (1996) 14 679.
[11] P. Bruno, C. Chappert, Phys. Rev. Lett. 67 (1991) 1602.
[12] M. van Schilfgaarde, F. Herman, Phys. Rev. Lett. 71 (1993) 1923.
[13] D. Venus, B. Heinrich, Phys. Rev. B 53 (1996) R1733.
[14] A. Davies, J.A. Stroscio, D.T. Pierce, R.J. Celotta, Phys. Rev. Lett. 76 (1996) 4175.
[15] B. Heinrich, J.F. Cochran, D. Venus, K. Totland, C. Schneider, K. Myrtle, J. Magn. Magn. Mater. 156 (1996) 215.
[16] J. Unguris, R.J. Celotta, D.T. Pierce, Phys. Rev. Lett. 69 (1992) 1125.
[17] D.T. Pierce, J.A. Stroscio, J. Unguris, R.J. Celotta, Phys. Rev. B 49 (1994) 14 564.
[18] Y. Wang, P.M. Levy, J.L. Fry, Phys. Rev. Lett. 65 (1990) 2732.
[19] Z.P. Shi, R.S. Fishman, Phys. Rev. Lett. 78 (1997) 1351.
[20] E.E. Fullerton, S.D. Bader, Phys. Rev. Lett. 77 (1996) 1382.
[21] A. Schreyer et al., Phys. Rev. Lett. 79 (1997) 4914.
[22] M.D. Stiles, J. Appl. Phys. 79 (1996) 5805.
[23] S.S.P. Parkin, Phys. Rev. Lett. 67 (1991) 3598.
[24] S.K. Kim et al., Phys. Rev. B 54 (1996) 5081.
[25] D.A. Tulchinsky, J. Unguris, R.J. Celotta, in preparation.
[26] A. Fuss, S. Demokritov, P. Grünberg, W. Zinn, J. Magn. Magn. Mater. 103 (1992) L221.
[27] M.E. Filipkowski, C.J. Gutierrez, J.J. Krebs, G.A. Prinz, J. Appl. Phys. 73 (1993) 5963.